



TMMOB ELEKTRİK MÜHENDİSLERİ ODASI  
İSTANBUL ŞUBESİ  
**2006-2007 ÖĞRETİM YILI PROJE  
YARIŞMASI**

**Name Of The Project : Maximum Power Point Tracker  
for PV Array**

**Owner of The Project : Kenan Askan**

**University : Istanbul Technical University  
Department of Electrical  
Engineering**

## **LIST OF CONTEST**

<b>Introduction.....</b>	<b>3</b>
<b>1.1 Photovoltaic System .....</b>	<b>6</b>
<b>1.2 Designing MPPT.....</b>	<b>11</b>
<b>1.2.1 Control circuit.....</b>	<b>11</b>
<b>1.2.2 Buck Converter.....</b>	<b>13</b>
<b>1.2.3 MPPT Algorithm Design.....</b>	<b>23</b>
<b>2. Conclusion and Future Works.....</b>	<b>31</b>
<b>References.....</b>	<b>32</b>
<b>Appendix.....</b>	<b>34</b>

## Introduction

Since both the world population and the industrialization growth dramatically, the world energy demand increases. To supply this demand, as energy source the fossil fuels are mostly used. However, it is fact that this source is going to be exhausted in the near future and generating energy from this source pollutes the environment. Due to that fact, the human kind is seriously concerned about that problem and looks for solution. The obvious and definite solution is generating energy from renewable sources such as sun, wind, hydrogen, etc, which are continuous forever and pollution free.

By using photovoltaic (PV) array, the sun light is converted to electricity. Photovoltaic sources are used today in many applications such as battery charging, water pumping, home power supply, swimming-pool heating systems, satellite power systems, automotive, etc. However, PV array are generally the bulkiest and most expensive parts of solar – powered electrical generation systems. Optimum utilization of available power from these arrays is therefore essential and can considerably reduce the size, weight, and cost of such power systems [1]. In order to acquire the optimization, the **Maximum Power Point Tracker (MPPT)** is required. Since the **Maximum Power Point (MPP)** of PV array is unique and changes as at least one of the irradiance, temperature, and load conditions (battery voltage) vary. MPPT is a microcontrolled based power electronic circuit that forces PV array to operate at its MPP point under all conditions which change the MPP of PV array.

A DC – DC step down chopper microcontroller based MPPT was designed for Istanbul Technical University 2007 Solar Powered Boat designed for 2007 SolarSplash competition taken place in Arkansas, USA. The boat has two configurations: sprint and endurance. In the sprint configuration where boats are supposed to race in a straight 300 meters track, within the limitation of battery (36 V) weight and capacity, and for maximum velocity, two PMG-132 brushed DC motors were selected to operate at 15 HP (See Figure 1 and 2). Moreover, the boat does not have to carry PV array and the batteries shall be charged by PV array. In endurance configuration, the boat has maximum 480 Watts PV array, 24 V batteries and 1 HP PMG132 permanganate DC motor (See Figure 3 and 4). This configuration consisted of PV array, MPPT, 24 V batteries, motor speed controller and PMG132 perm DC motor. The all endurance configuration is showed in Figure 5.

Since, according Solar Splash 2007 rules, sunlight is the only power source for charging energy storage devices used for propulsion of boat, the obtaining MPP of PV array is the essential for efficiency and power management of boat. Due to that fact, the MPPT designed and built for ITU Solar Powered Boat designed for 2007 Solar Splash.

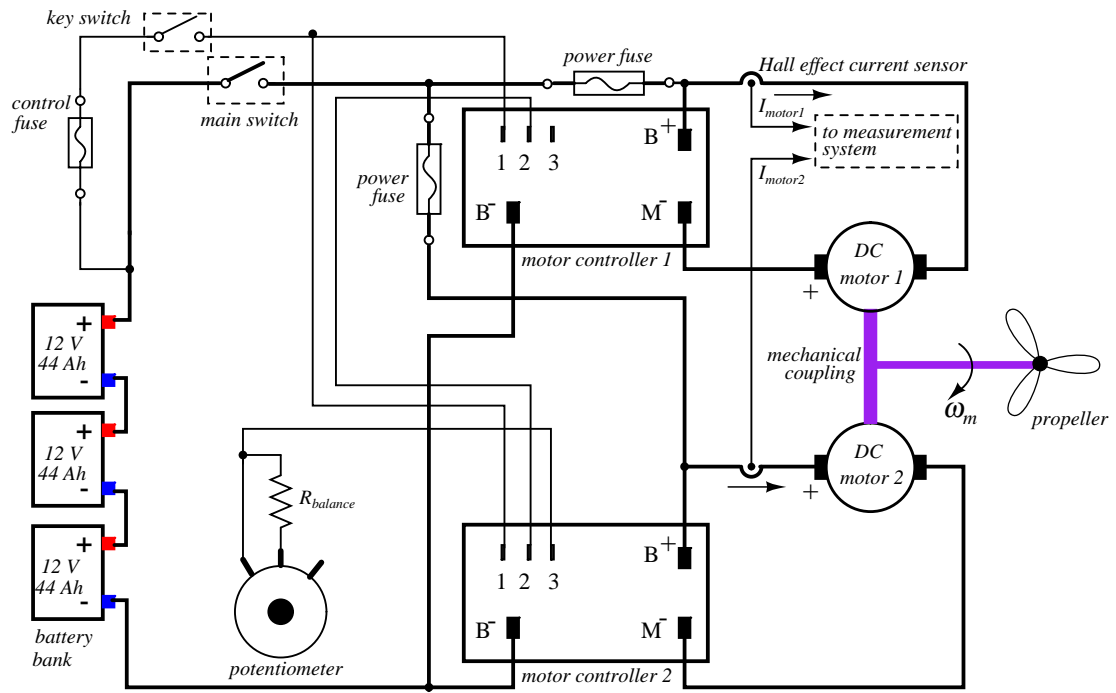


Figure 1: Sprint Electrical Configuration

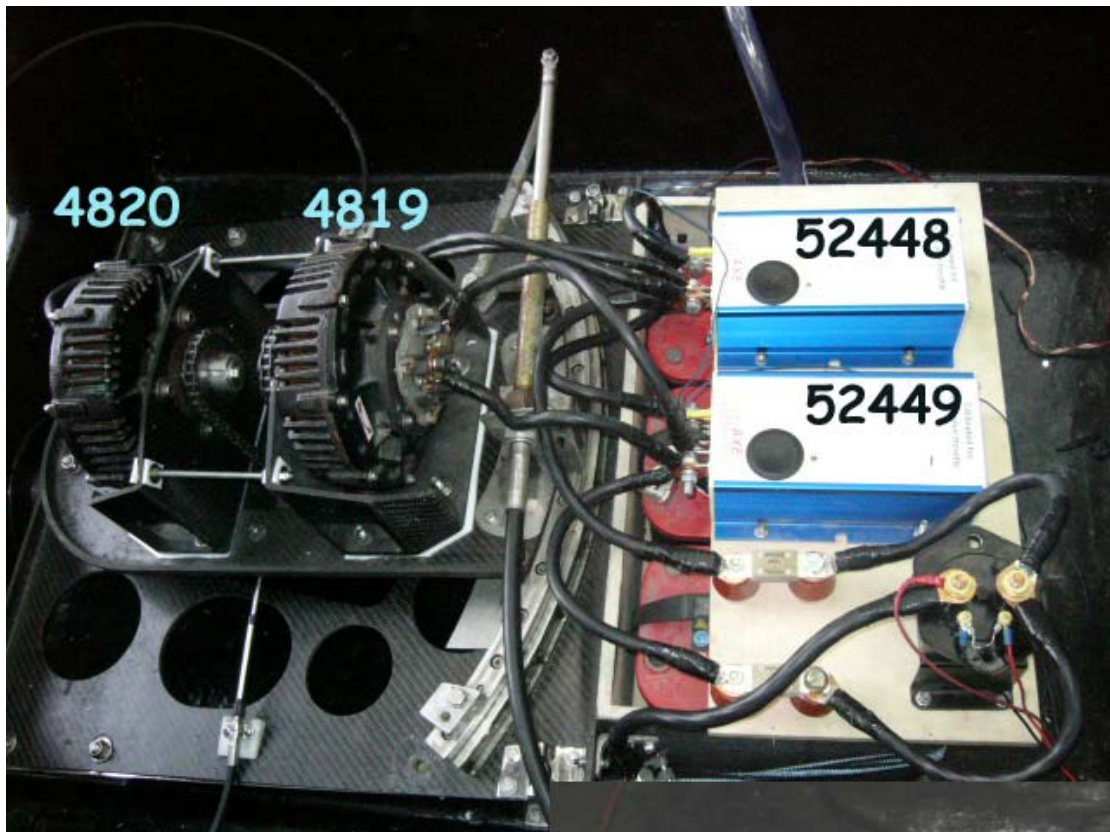


Figure 2: Sprint Electrical Configuration

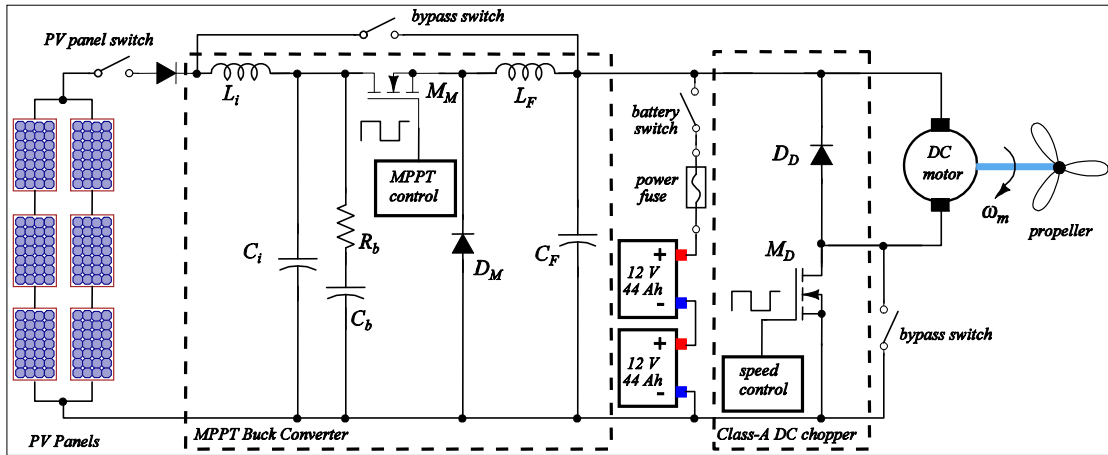


Figure 3: Endurance Configuration

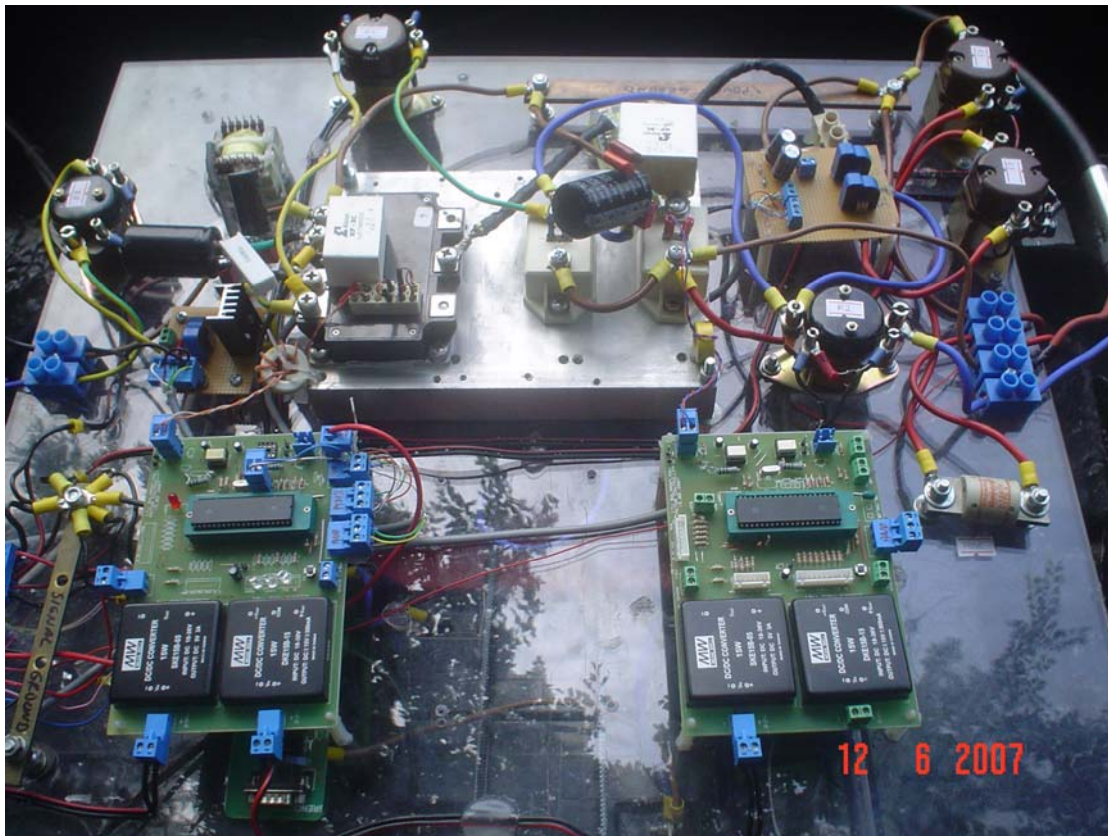


Figure 4: Endurance Configuration



Figure 5: All Endurance Configurations

### 1.1 Photovoltaic System

According to Solar Splash rules, sunlight is the only power source for charging energy storage devices used for propulsion of boat. The sunlight will be converted to electrical energy by solar cells. The energy delivered by photovoltaic (PV) arrays is stored in lead-acid batteries or directly used for propulsion of the boat. The output power ( $P_{out}$ ) of PV arrays may not have a one sun output greater than 480 watts and open circuit voltage ( $V_{oc}$ ) can not be greater than 52 V. During competition, PV arrays are used to charge sprint and endurance batteries and used for endurance lap.

PV arrays are generally the bulkiest and most expensive parts of solar – powered electrical generation systems. Optimum utilization of available power from these arrays is therefore essential and can considerably reduce the size, weight, and cost of such power systems [1]. By regarding this fact and considering requirements included  $P_{out}$ , area,  $V_{oc}$ , short circuit current ( $I_{sc}$ ), peak power voltage ( $V_{MPP}$ ), peak power current ( $I_{MPP}$ ), fill factor (FF), being currently available and cost, the best appropriate design was determined after long searches.

A – 300, mono crystalline silicon solar cell manufactured by Sunpower Corporation is used. The A -300 supplies all requirements indicated above. The required characteristics of A – 300 are showed in Table 1. The array is divided into six sections of 28 cells each, having a voltage rating of 16 V. Three sections will be placed in series to achieve a total array voltage of 48 V. The array calculations show an overall output of 521 W. This is above the maximum allowed output, but was chosen as such to overcompensate for approximately 10% loss in

reflected photons due to the lamination technique used to protect the cells [2]. This design is shown below in Figure 6.

Table 1: Characteristic of A – 300 Cells

Open Circuit Voltage	Short Circuit Current	Maximum Power Voltage	Maximum Power Current	Rated Power	Efficiency Maximum
0.670 V	5.9 A	0.560 V	5.54 A	3.1 W	21.5%

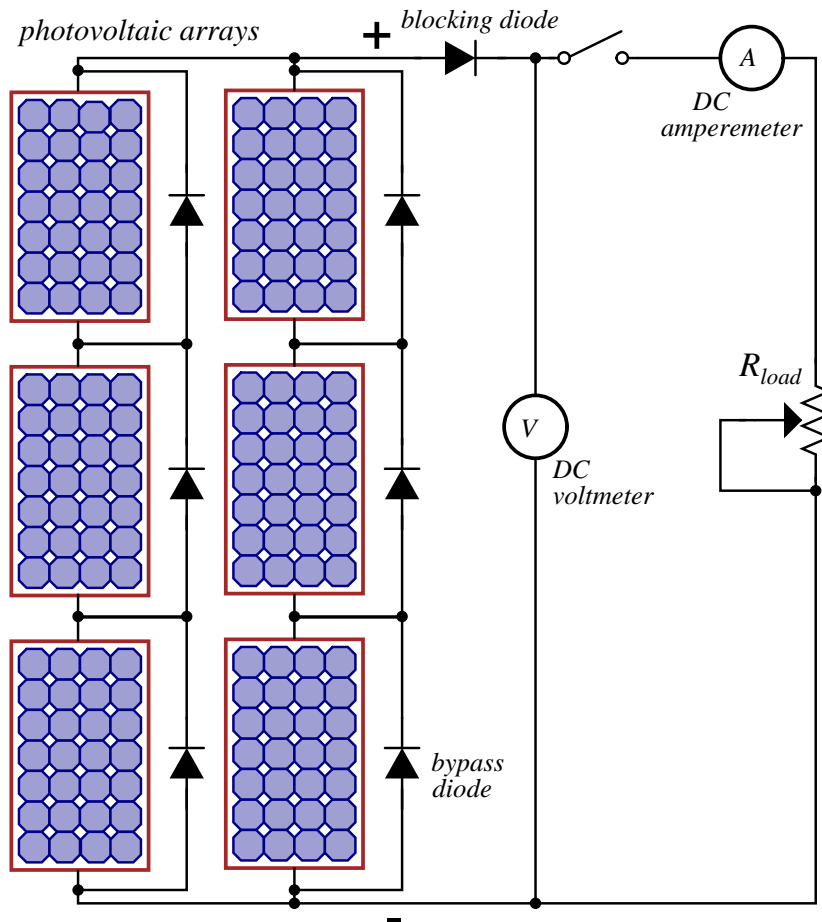


Figure 6: Solar Array Design and Determining I – V Curve

In order to determine I – V curve of PV array, an adjustable resistor was connected across the array (See Figure 6 and 7). As resistance was varied, the currents and voltages were obtained. By drawing the data, I – V curve of PV array was obtained (See Figure 8).



Figure 7: Determining Characteristic of PV array

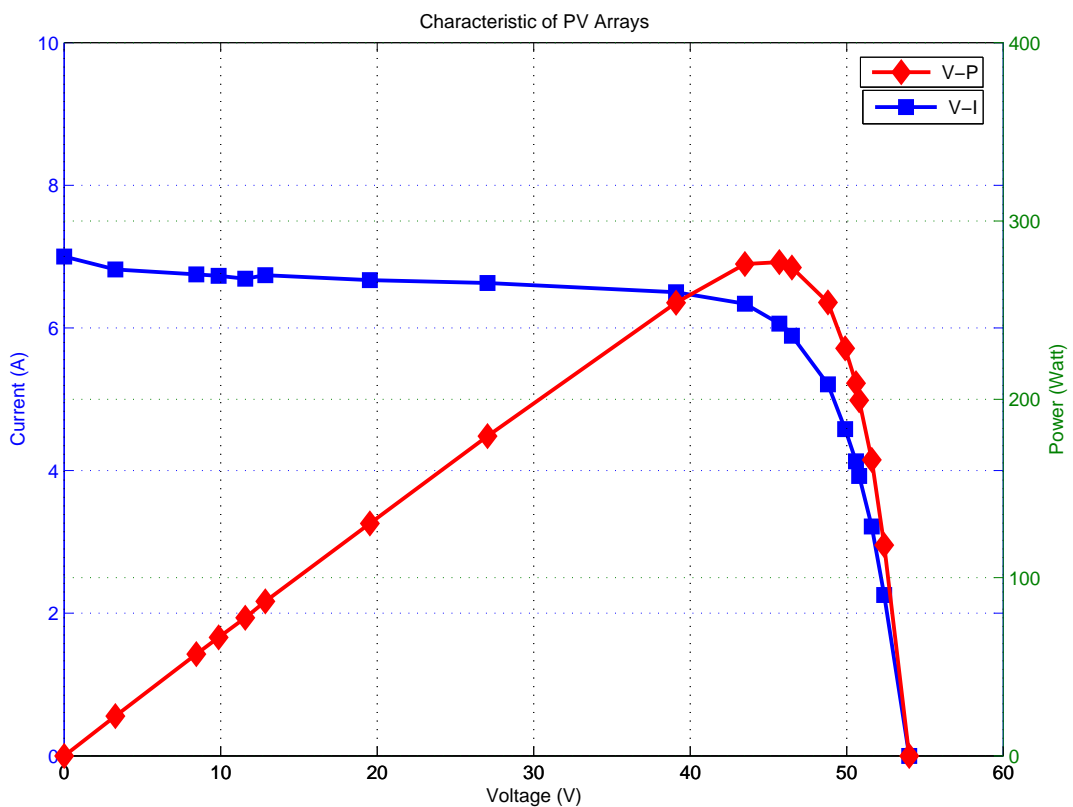


Figure 8: I - V, P - V Curve of PV array

As can be seen on Figure 8, the maximum power point (MPP) of PV array is at the knee of I - V curve and it is a unique point. Moreover, since solar cells are semiconductor devices, the power delivered by the PV array depends on the irradiance, temperature, and load conditions (battery voltage). As these parameters constantly change during daytime, the

current – voltage (I - V) characteristic of PV arrays varies (See Figure 9, 10 and 11). Due to that fact, if the PV is directly connected to load even at its MPP, it may not operate at its MPP. Therefore, the required power will not be obtained from PV array. Instead a power electronic circuit called maximum power point tracker (MPPT) is located between solar panel and load. In other word, if the PV array is connected to load directly, as it is seen from Figure 12, the PV array doesn't operate at its MPP. Therefore, around 34 % power loss occurs [3]. On the contrary, by using MPPT, the PV array operates at its MPP and no power losses appear (See Figure 13).

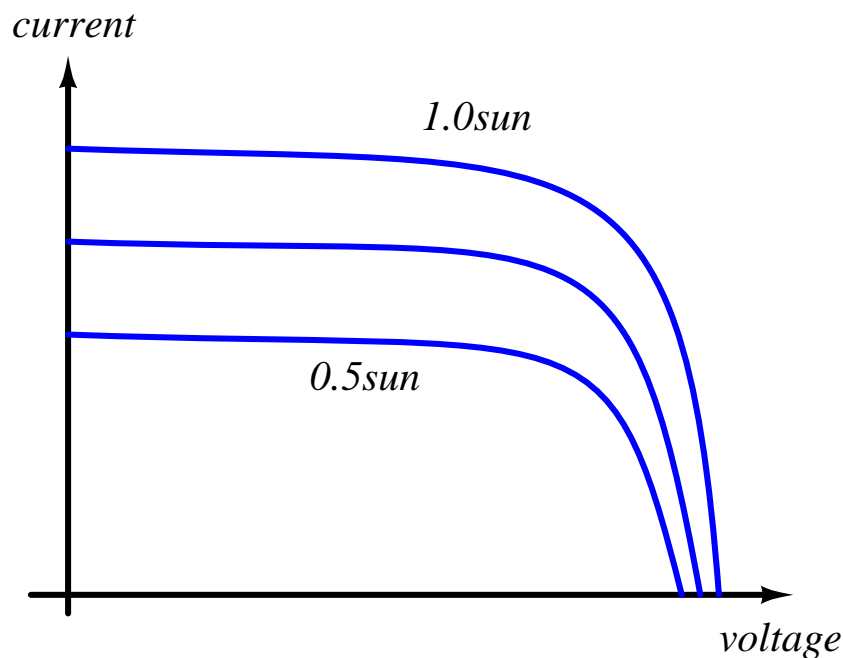


Figure 9: Maximum Power of PV Array with Different Solar Irradiances

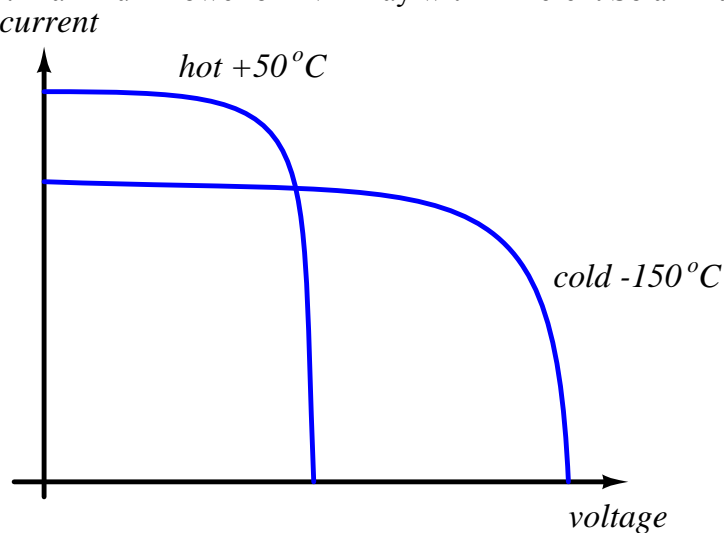


Figure 10: Different I – V curve at different temperatures

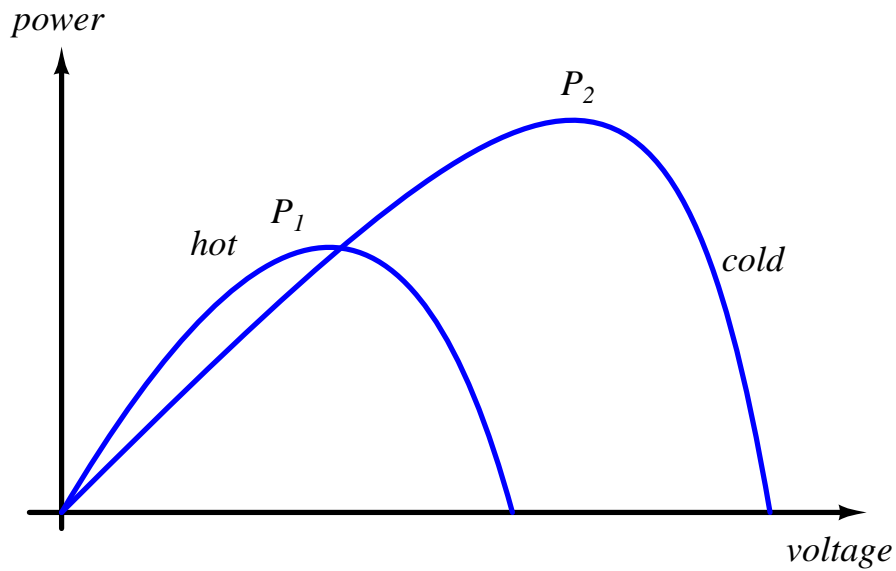


Figure 11: Different P – V curve at different temperatures

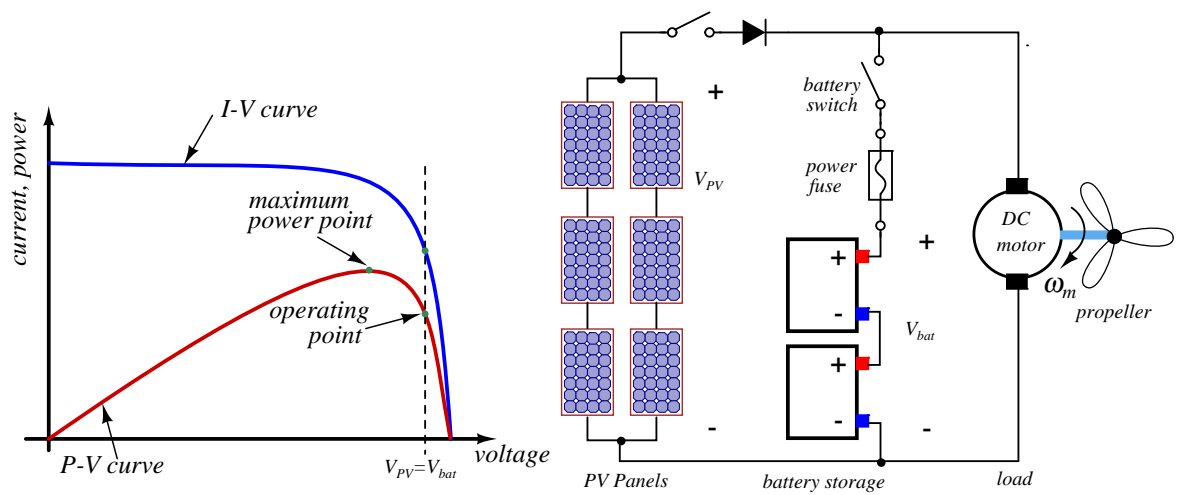


Figure 12: The solar cells system without MPPT

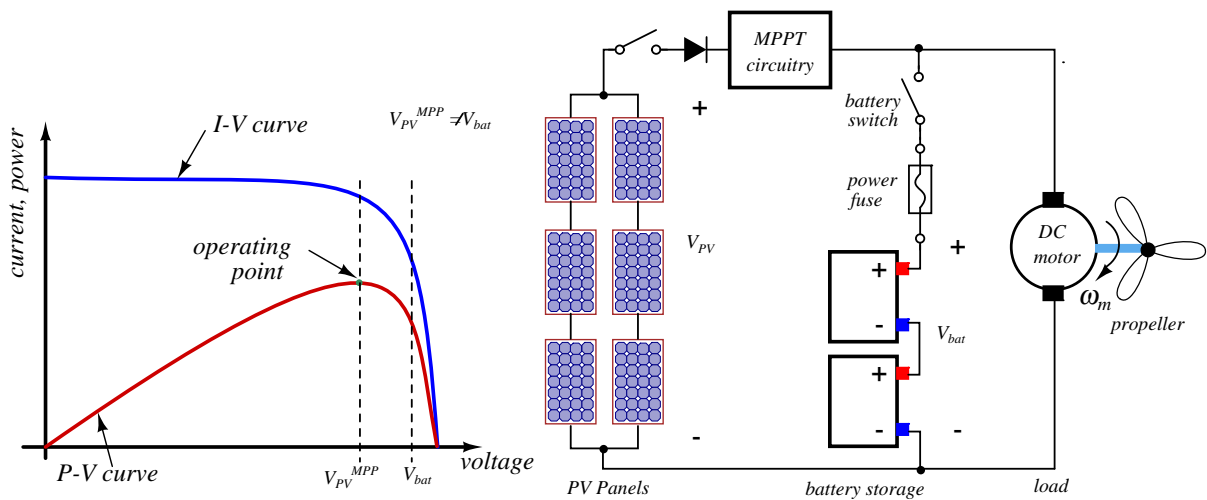


Figure 13: The solar cells system with MPPT

MPPT is a microcontroller based, high switching frequency, DC – DC converter that forces PV array to operate at its MPP under both changeable atmospheric conditions and load voltage situation. As battery voltage (24V) is less than PV voltage (48V), a buck (step - down) converter is used. The analog signals such as voltage and current sampled by control circuit of MPPT are converted to digital signal by internal analog to digital converter (ADC) of microcontroller in order to be used in MPPT algorithm. Then, according to the result of MPPT algorithm, the duty cycle of buck converter is determined to operate PV array around MPP.

## 1.2 Designing MPPT

The required operating characteristics of MPPT developed by electrical team calling **Nusrat Maximum Power Point Tracker (NuMPPT)** for Solar Splash 2007 Endurance lap are listed in Table 2. Design and build process of MPPT consisted of improving control circuit, determining the most efficient buck converter (DC – DC chopper) configuration, reliable measurement system, and improving control algorithm, respectively.

Table 2: Designed MPPT Characteristics

<b>Switching frequency</b>	<b>Input Current Range</b>	<b>Output Current Range</b>	<b>Input Voltage Range</b>	<b>Output Voltage Range</b>	<b>Power Range</b>
20 kHz	0 – 15 A	0 – 30 A	0 – 55 V	0 – 40V	0 – 600 W

### 1.2.1 Control circuit

The multipurpose control circuit where PCB schematics and the picture of the real circuit are shown in Figures 14 and 15, respectively. This control board is designed and produced by the electrical team. Two on board isolated flyback DC-DC converters are used to convert incoming battery voltage to 5V required by the microcontroller and to 15V required by the isolated optocoupler driver. These converters can operate for input voltages between 18 V and 36 V. The reason for employing two isolated power supplies is that the grounds of microcontroller and measurement circuits must be different than the source terminal of MOSFET in the buck converter of NuMPPT.

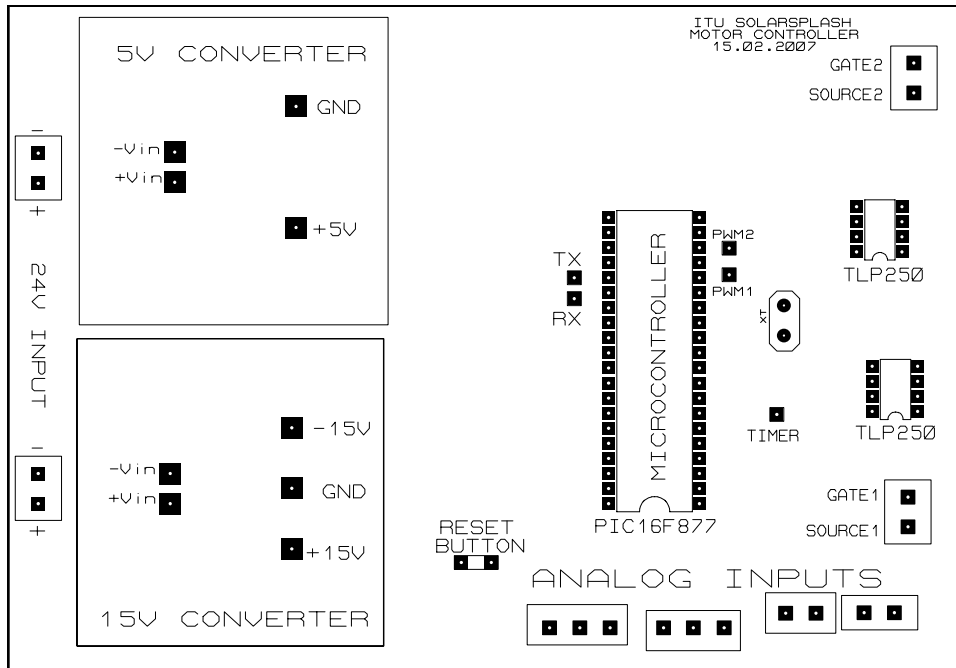


Figure 14: PCB schematics of control circuit



Figure 15: Multipurpose Control Circuit

All analog inputs of the microcontroller (AN0-AN7) have 5.1 V zener diode protections. On the board, there are two LED indicators, one seven segment display output, serial communication outputs (TX, RX) and other input/output pins. Two PWM outputs of microcontroller are connected to the input of the optocouplers on the board. Same circuit board is used as NuMPPT control circuit, NuMC and telemetry system. Dimensions of the board are measured as 16 cm wide and 11 cm high. Using same circuit for different purposes simplifies the electrical team's work in terms of the material inventory and backup. The photo of the circuit is shown in Figure 15.

To generate a variable duty cycle PWM signal, PIC16F877 microcontroller throttle position is divided into ten equal levels which make 10% speed change. With a basic analog-to-digital conversion, this position changes converted to register values which adjusts duty cycle of the control signal. The frequency of PWM signal set to 20 kHz outside the audible range of human ear.

Gate signal of the MOSFET is produced by using PIC16F877 microcontroller in the control circuit. Since output current source capability of microcontrollers are not sufficient enough to charge and discharge of gate-source capacitance, an optocoupler is employed to drive the MOSFET – providing fast turn-on and turn-off times. Duty cycle of gating signal controlled by a ten-step throttle determines the motor speed.

Any two adjacent conductors can be considered as a capacitor, although the capacitance will be small unless the conductors are close together or long. This (unwanted) effect is termed "stray capacitance" [4]. When MOSFET is switching at high speeds, current spikes occur at high frequencies because of MOSFET drain-to-heatsink capacitance, called stray capacitance. Providing a short path for the current to return to its origin, adding common-mode filters and slowing down the switching time are ways to avoid from these current spikes [5]. Because of presence of stray inductances and fast switching of current signals ( $L_{stray} di/dt$  induced voltages), unwanted voltage and current spikes/oscillations were observed during testing in various part of the circuit. To protect MOSFET and diode from overvoltages exceeding its rated values, snubber circuits are employed. The snubber circuit of chopper is a common mode filter. This filter includes some snubber elements which were used between drain and ground (source). To reduce the coupling of unwanted signals to the control circuit, short, twisted and shielded wires are used. These wires are also passed through a ferrite toroid for several turns to reduce the effect of common-mode noises.

In order to program NuCC for required purpose, C programming language is used and HI – TECH PIC C 8.02PL is used as compiler. Since, its own editor operates on command windows; it does not handle to work quickly. Therefore, it was integrated into Microchip MPLAB 7.31 and the code is written in MPLAP's editor. The codes can be seen at Appendix.

### 1.2.2 Buck Converter

A buck converter was designed for the solar powered boat because battery voltage is lower than the array voltage. Battery voltage is around 24V and PV array voltage is about maximum 48V. A buck converter is a DC – DC step down converter that accepts PV arrays voltage to produce lower DC voltage, generally equals to battery voltage. The buck converter topology is shown in Figure 16.

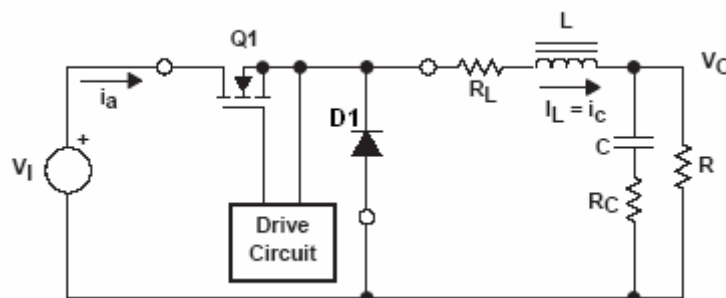


Figure 16: A buck converter topology

Q1 is the main switch that is MOSFET, D1 is freewheeling diode, L and  $R_L$  are inductor and its series resistor, C and  $R_C$  are capacitor and its equivalent series resistor (ESR). Drive circuit controls the power transfer to the load R by adjusting on-off time of Q1. The buck converter operation is divided in two categories: Continuous and discontinuous mode.

In the continuous mode, the converter has two states per period. For one state, Q1 is “on” and D1 is “off”, for another state, Q1 is “off” and D1 is “on”. When Q1 is on, the buck converter looks like in Figure 17 and equations for this state are as follows:

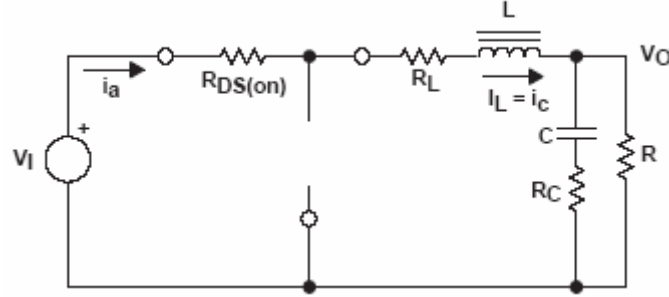


Figure 17: Q1 “on” state

$$V_L = V_I - V_O \text{ and } L \frac{di}{dt} = V_I - V_o$$

$$\frac{di}{dt} = \frac{V_I - V_O}{L} = \frac{\Delta i_1}{DT} \quad (1.1)$$

$$\Delta i_1 = \frac{(V_I - V_O)}{L} * DT \quad (1.2)$$

When Q1 is off,

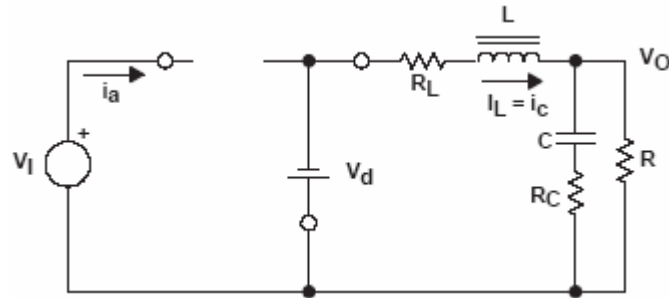


Figure 18: Q1 “off” state

$$V_L = -V_O = L \frac{di}{dt} \quad (1.3)$$

$$\frac{\Delta i_2}{(1-D)T} = -\frac{V_O}{L} \quad (1.4)$$

$$\Delta i_2 = -\frac{V_O(1-D)T}{L} \quad (1.5)$$

Figure 19 shows diode current, MOSFET current, inductance and output current waveforms for continuous mode buck converter.

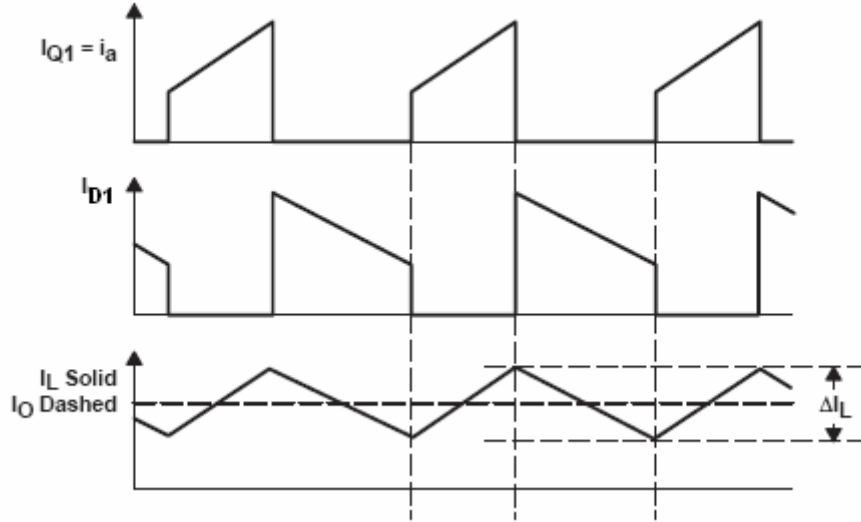


Figure 19: Current waveforms for continuous mode

Net inductor current change at steady state operation is zero per period. Therefore, when Eq. 1.2 and 1.5 are used,

$$|\Delta i_1| = |\Delta i_2| \quad (1.6)$$

$$\frac{(V_1 - V_o)}{L} DT = \frac{V_o(1-D)T}{L} \quad \text{and as a result,}$$

$$V_o = DV_1 \quad (1.7)$$

After some calculations, if voltage drops at MOSFET, diode, inductor and capacitor are included, the overall equations are obtained for continuous mode.

Table 3: Continuous Mode Buck Converter Equations

$\Delta V_o = \frac{(V_o + V_D + V_{RL})(1-D)}{8LCf^2}$	$\Delta i = \frac{(V_o + V_D + V_{RL})(1-D)}{2fL}$
$I_{\max} = \frac{2V_oLf + (V_o + V_D + V_{RL})(1-D)R}{2LRf}$	$I_{\min} = \frac{2V_oLf - (V_o + V_D + V_{RL})(1-D)R}{2LRf}$
$L_{\min} = \frac{(V_o + V_D + V_{RL})(1-D)R}{2fV_o}$	$D = \frac{V_o + V_{RL} + V_D}{V_1 - V_o + V_D}$

In the discontinuous mode, inductor current becomes zero before the next switching begins. The discontinuous mode has three stages: For one state Q1 is “on” and D1 is “off”, for second state Q1 is “off” and D1 is “on”, for the last state Q1 and D1 is “off” during current becomes zero. While the buck converter is operating in the continuous mode, if load current decreases, the converter changes its operation to the discontinuous mode. Also, there is a boundary between the continuous and discontinuous modes. At this boundary, after inductor current is zero, the next switching cycle begins increasing again as shown in Figure 20.

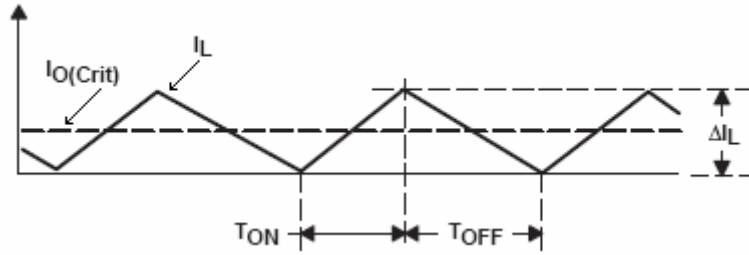


Figure 20: Boundary condition

If current continues to decrease, then the discontinuous mode occurs. Figure 21 shows the discontinuous mode.

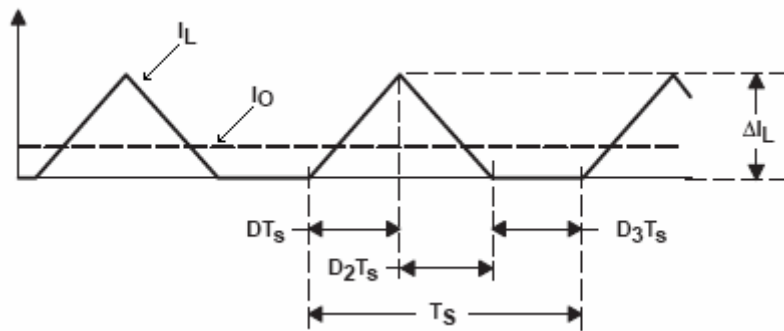


Figure 21: The discontinuous mode

For the stability operation, the critical inductance value must be determined since frequency response is different from the continuous mode in the discontinuous mode. When  $I_{\min}=0$ , the critical inductance value is determined.

$$I_{\min} = 0 = V_o \left[ \frac{1}{R} - \frac{(1-D)}{2Lf} \right]$$

$$L_{\min} = \frac{(1-D)R}{2f} \quad (1.8)$$

### 1.2.2.1 MOSFET And Diode Selection

Referring to  $V_{in}$  and  $I_a$  values, MOSFET and freewheeling diode elements are selected. As a 48V source voltage and approximate 12 A current flows through the load, Mitsubishi FM600TU-07A MOSFET module is a proper element for buck converter. This module can be used up to maximum 75 V drain-source voltage and 300 A for the drain current. The strongest characteristic of the module is drain-source resistance ( $R_{ds(on)}$ ). Module has maximum 0.73 mΩ  $R_{ds(on)}$  resistance. Moreover, as the freewheeling diode, same MOSFET's internal inverse diode chosen. This diode can operate up to 300 A, has maximum 0.8 V voltage drop on it and 200 ns reverse recovery time.

### 1.2.2.2 Inductor Design

The filter inductor was designed by using  $K_g$  method.  $K_g$  Method is defined as magnetic size of core for a given copper loss and  $B_{\max}$ . Initially, some parameters like inductance value

$L$ , peak winding current  $I_{\max}$ , maximum flux density  $B_{\max}$ , wire resistivity ( $\rho$ ), and winding resistance  $R$  are required to design inductor. It is important to use low winding resistance and to avoid from saturation. Most core types have air gap that prevents saturation of core. The remanens flux density  $B_r$  has high value without air gap and this causes voltage spikes in the converter.

The minimum critical value of inductance,

$$L_{\min} = \frac{(V_O + V_D + V_{RL})(1-D)R}{2fV_O}$$

First of all, we can assume that MOSFET voltage drop and inductance voltage drop are zero and then, the result of value is multiplied by a constant to approach precise value.

$$V_O = 24V$$

$$D = \frac{V_O}{V_{IN}} = \frac{24}{40} = 0.6$$

$$R = \frac{V_O}{I_O} = \frac{24}{20} = 1.2$$

$$f = 20kHz = 20000Hz$$

As a result, the minimum value of inductance equals to,

$$L_{\min} = \frac{(24 + 0 + 0)(1 - 0.6)1.2}{2 * 20000 * 24}$$

$$L_{\min} = 12 \mu H$$

If the MOSFET voltage drop and inductance voltage drop were considered, the minimum inductance value would be,

$$V_D = I_O \cdot R_{DSon} = 20 \cdot 0.007 = 0.14V$$

$$V_{RL} = I_O \cdot R_L = 20 \cdot 0.05 = 1V$$

$$L_{\min} = \frac{(24 + 0.14 + 1)(1 - 0.6) \times 1.2}{2 \cdot 20000 \cdot 24}$$

$$L_{\min} = 12.56 \mu H$$

If the nominal value of inductance is selected as,

$$L = 8 \cdot L_{\min} = 100 \mu H$$

then current ripple becomes,

$$\Delta i = \frac{(24 + 0.14 + 1)(1 - 0.6)}{2 \cdot 20000 \cdot (50 \cdot 10^{-6})} = 5.028A$$

This current ripple is reasonable value for 20-A output current

The second required parameter for inductor design is maximum flux density ( $B_{\max}$ ).  $B_{\max}$  should be chosen a value that is less than the saturation flux density  $B_{sat}$ .  $B_{\max}$  was selected 0.25 Tesla for EE core.

The third required parameter is maximum current that passes through inductor winding is calculated as,

$$I_{\max} = I_o + \Delta i$$

$$\Delta i \leq 3A$$

Then the maximum current is calculated as,

$$I_{\max} = 20 + 3 = 23A$$

Another parameter is winding resistance. Winding resistance can be determined by copper loss. In such a manner that 1-W copper loss is good solution for converter efficiency. Therefore,

$$P_{\text{loss}} \leq 1W$$

$$I_L^2 \cdot R \leq 1$$

$$R \leq \frac{1}{20^2} = 0.0025\Omega$$

or resistance can be calculated as,

$$R = \frac{\rho \cdot l}{A_w} \quad (1.9)$$

where  $\rho$  is the resistivity,  $l$  is the length of wire. The length of wire can be expressed as,

$$l = (MLT) \cdot n \quad (1.10)$$

where  $(MLT)$  is the mean-length-per-turn of the winding. As a result, if Eq. 1.9 and 1.10 are used, winding resistance equals to

$$R = \frac{\rho \cdot (MLT) \cdot n}{A_w} \quad (1.11)$$

The last required parameter for inductor design is winding area. The winding of inductor must be suitable for the hole in the center of the core. If the winding has  $n$  turns and the cross-sectional area is  $A_w$ , then total copper area in the center will be

$$S_w = A_w \cdot n$$

When the hole area is  $W_A$  and copper area is  $A_w$ , the available conductor area is,

$$K_u \cdot W_A$$

where  $K_u$  is called fill factor which is between 0 and 1.

$$K_u = 0.5 \text{ for a simple low voltage inductor}$$

$$K_u = 0.25 - 0.3 \text{ for an off-line transformer}$$

$$K_u = 0.05 - 0.2 \text{ for a high voltage transformer}$$

$$K_u = 0.65 \text{ for a low voltage foil inductor or transformer}$$

Therefore, the relationship between the hole area and copper area is,

$$A_w \cdot n \leq K_u \cdot W_A \quad (1.12)$$

and using Eq. 4.12,

$$\frac{A_{C^2} \cdot W_A}{(MLT)} \geq \frac{\rho \cdot L^2 \cdot I_{\max}^2}{B_{\max}^2 \cdot R \cdot K_u} \quad (1.13)$$

where  $A_C$  is core area. Left side of inequality that is called as the core geometrical constant ( $K_g$ ) is composed of unknown parameters whereas right side of inequality is composed of known parameters. So,

$$K_g \geq \frac{\rho \cdot L^2 \cdot I_{\max}^2}{B_{\max}^2 \cdot R \cdot K_u} \cdot 10^8 \quad (cm^5) \quad (1.14)$$

All input parameters are shown in Table 4.

Table 4: Input parameters for  $K_g$  method

Inductance [L]	Maximum flux density [ $B_{\max}$ ]	Wire resistivity [ $\rho$ ]	Maximum current [ $I_{\max}$ ]	Winding resistor [R]	Fill factor [ $K_u$ ]
50 $\mu$ H	0.25 T	$1.724 \cdot 10^{-6} \Omega \text{ cm}$	23 A	0.0025 $\Omega$	0.5

The wire resistivity is  $1.724 \cdot 10^{-6} \Omega \text{ cm}$  for copper at room temperature and was added to Table 4.

The first step is to determine core size by using Eq. 1.14. for inductor design.

$$K_g \geq \frac{1.724 \cdot 10^{-6} \cdot (50 \cdot 10^{-6})^2 \cdot 23^2}{0.25^2 \cdot 0.0025 \cdot 0.5} \cdot 10^8$$

$$K_g \geq 2.91838 \quad (cm^5) \quad (1.15)$$

According to ferrite catalogs, EE70/68/19 core type has a convenient geometrical constant that is 5.06. For this core,

$$A_C = 3.24 \text{ cm}^2$$

$$W_A = 6.75 \text{ cm}^2$$

$$MLT = 14 \text{ cm}$$

Table 5: EE70/68/19 core data

Cross-sectional area $A_c$ [ $\text{cm}^2$ ]	Hole area $W_A$ [ $\text{cm}^2$ ]	Mean length per turn $MLT$ [cm]	Core weight [g]
3.24	6.75	14	280

The second step is to determine air gap length by using Eq. 1.16.

$$l_g = \frac{\mu_0 \cdot L \cdot I_{\max}^2}{B_{\max}^2 \cdot A_C} \cdot 10^4 \quad (\text{m}) \quad (1.16)$$

where  $\mu_0$  is the permeability of free space.

$$l_g = \frac{(4\pi \cdot 10^{-7}) \cdot (50 \cdot 10^{-6}) \cdot 23^2}{0.25^2 \cdot 3.24} \cdot 10^4$$

$$l_g = 1.641 \text{ mm}$$

The third step is to determine number of turns by using Eq. 1.17.

$$n = \frac{L \cdot I_{\max}}{B_{\max} \cdot A_C} \cdot 10^4 \quad (1.17)$$

$$n = \frac{(50 \cdot 10^{-6}) \cdot 23}{0.25 \cdot 3.24} \cdot 10^4$$

$$n = 14.19 = 14 \text{ turns}$$

The last step is to determine wire size by using AWG data and Eq. 1.18

$$A_w \leq \frac{K_u \cdot W_A}{n} \quad (\text{cm}^2) \quad (1.18)$$

$$A_w \leq \frac{0.5 \cdot 6.75}{14}$$

$$A_w \leq 2.41 \quad (\text{cm}^2)$$

According to AWG data, AWG #24 is suitable for the inductor. Some properties of copper are as follows:

$$A_w = 2.047 \quad (\text{cm}^2)$$

$$\text{Diameter} = 0.0566 \text{ cm}$$

Finally, the inductor was assembled by a transformer company (Elektra Transformer) and its properties are shown in Table 6 while the picture of the inductor is illustrated in Figure 22.

Table 6: Features of designed inductor

Core Type	Wire size [# AWG]	Number of turns	Air gap length [mm]
EE70/68/19	24	14	1.641

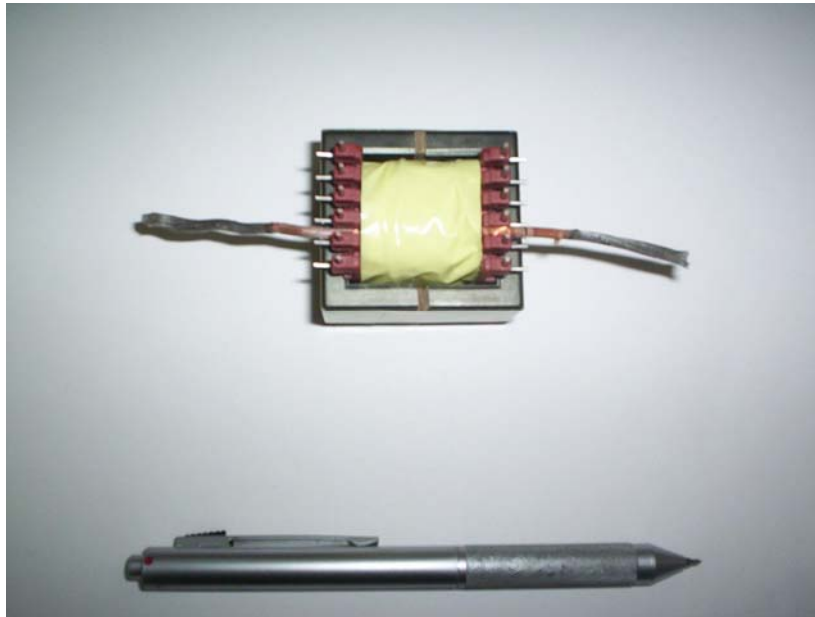


Figure 22: Picture of the inductor.

### 1.2.2.3 Protection Issues: Snubber Circuits:

In order to limit the voltage appearing across the switching devices during MOSFET turn-off, additional protection circuitry called snubber circuits was needed. Snubbers are protection elements consisting of a series connected resistor and capacitor, connected directly between positive-negative terminals of MOSFET. Figure 23 shows the voltage across MOSFET for a duty cycle of 50%. It is clear from this graph that MOSFET is subjected to a voltage stress of 75V for a 45 V supply voltage – nearly three times the supply voltage. This short duration spike is very close to the rated voltage of the MOSFET module (75V). A snubber circuit is placed across the power MOSFET to limit the rate of rise of voltage during turn-off. The results of the MOSFET voltage after the snubber circuit is placed are given in Figure 24 where the maximum value of voltage is reduced to half of the previous value.

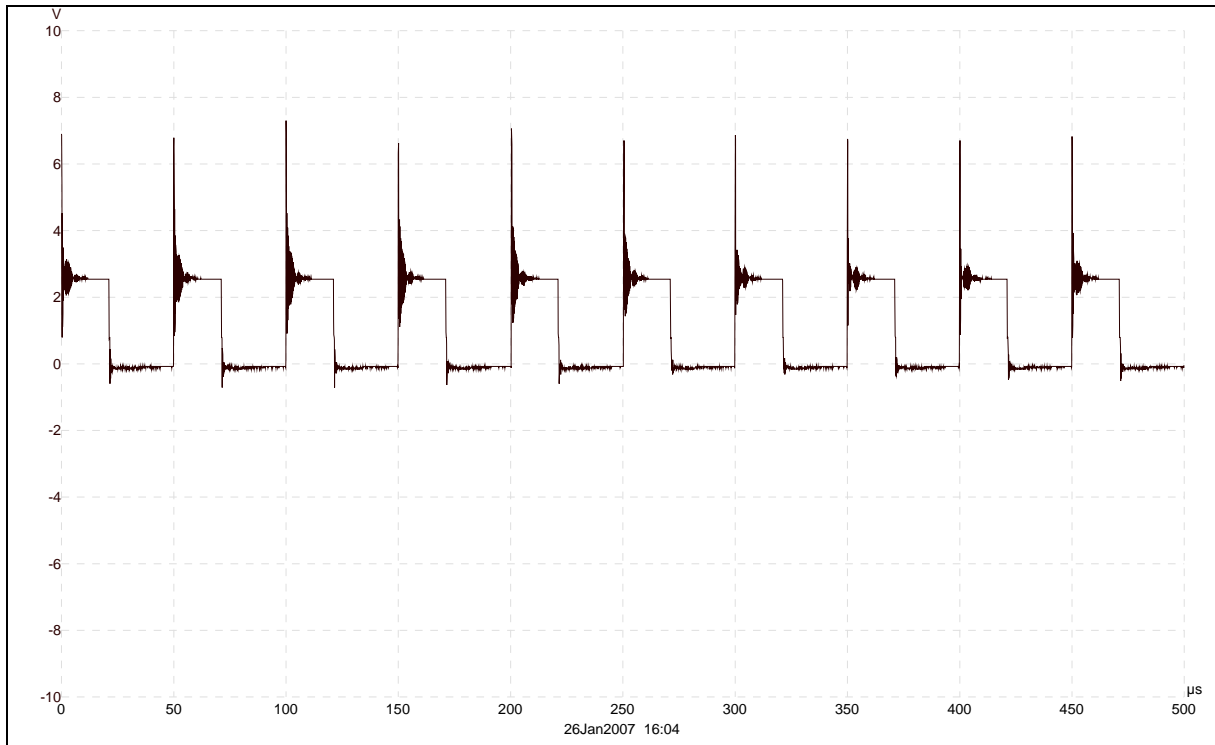


Figure 23: Voltage across MOSFET during turn off instants before snubber circuits are employed (y axis scale is 20 V/div, time axis 50  $\mu\text{s}/\text{div}$ ).

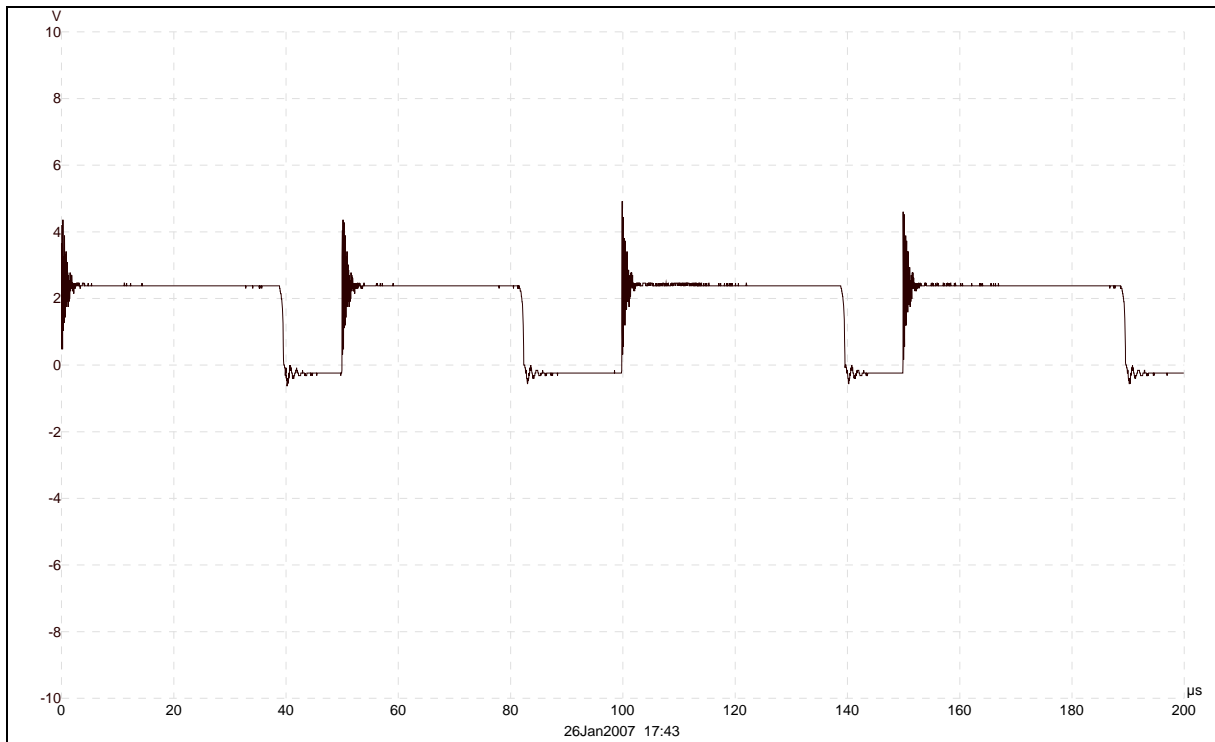


Figure 24: Voltage across MOSFET during turn off instants after snubber circuits are placed (y axis scale is 20 V/div, time axis 20  $\mu\text{s}/\text{div}$ ).

### 1.2.3 MPPT Algorithm Design

The most essential part of MPPT is its control algorithm. MPPT algorithm increases or decreases duty cycle in order to determine MPP as the operating conditions change which causes the maximum power point of PV array vary. Since the MPP of PV array is just only one point on V- P curve, the algorithms used should operate efficiently as much as it is possible to operate the PV array at this point.

By considering this fact, the various algorithms were tested to determine the most efficient methods. Before testing conventional MPPT methods, the PV array operated at its MPP by manually adjusting duty cycle of buck converter to monitor MPP points during atmospheric condition changes. The test started on April 12, 2007 at 11:15 am and finished at 15:50 pm. During test, PV voltage ( $V_{pv}$ ), current ( $I_{pv}$ ) and  $P_{out}$  were measured at 4 minutes interval periodically. Moreover, the weather was sunny and there were some cloud passing. The temperature was almost same during test. The test results are showed in Figure 25

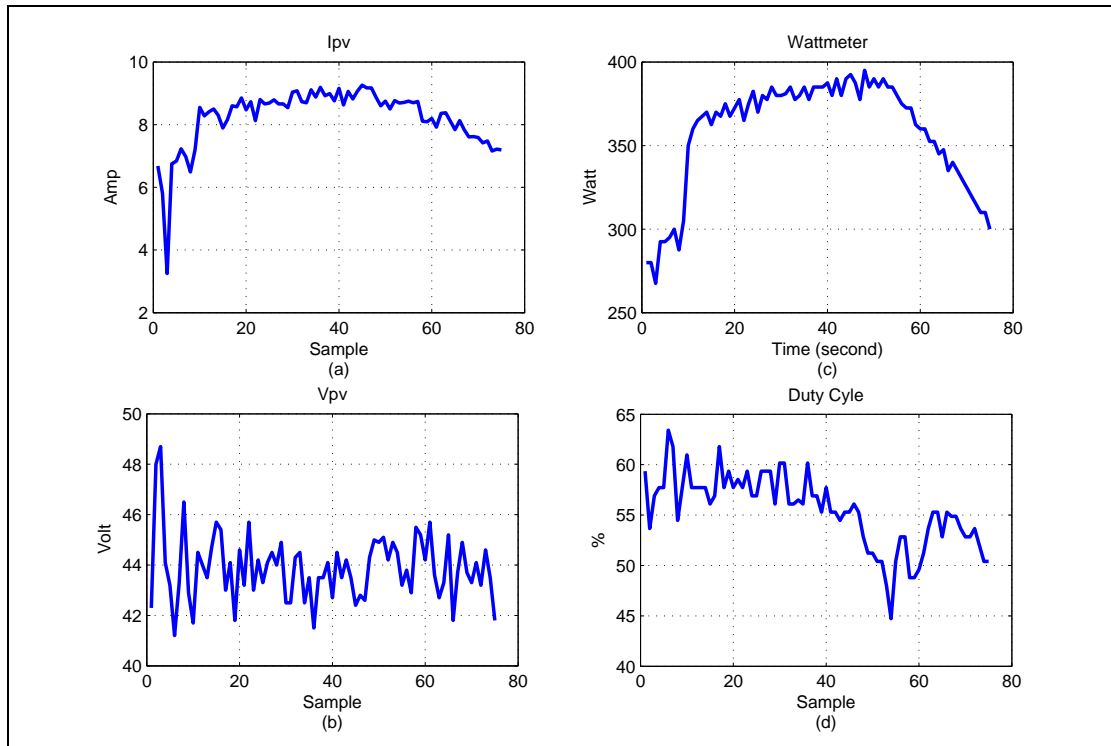


Figure 25: PV Array Maximum Power Points during Test

According to the measured data, the average,  $I_{MPP}$  and  $P_{MPP}$  are 44.5V, 8.23A and duty cycle was 56%, respectively. It is seen from Figure 25 that, as irradiance increases, the PV voltage decreases and current increases. Moreover, the MPP is fluctuated during testing. It could depend on cloudy time, partial shadowing and load demand. In additional, during testing the temperature was measured and no considerable differences recognized (temperature is assumed to be constant). It is therefore concluded that the temperature did not affect MPP seriously. Beside, the PV array operating environment on the craft is not subject to great temperature differences (See Figure 26). Moreover, it was recognized that the solar irradiance is maximum at noon (See Figure 25 (b) and Figure 27).



Figure 26: Solar Array Environment on Boat

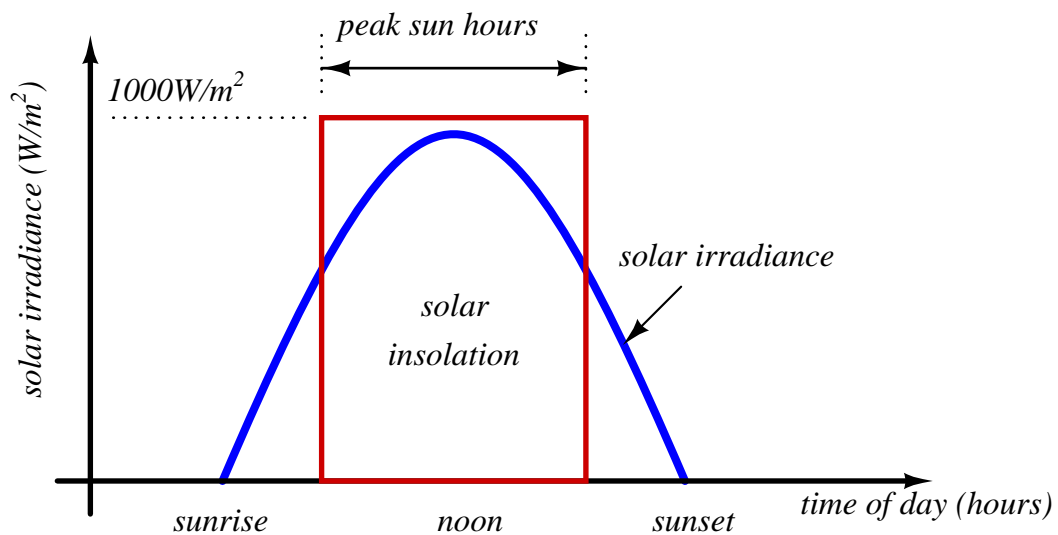


Figure 27: Solar irradiance changes during the day

Also, the temperature coefficients for A – 300 are  $-1.9 \text{ mV}/^{\circ}\text{C}$  and  $-0.38\%/^{\circ}\text{C}$ . Consequently, by considering all conditions, it was decided that the effect of temperature on MPP is not a major consideration for MPPT algorithm.

While deciding to choose the best algorithm for the solar boat application, ease of implementation, using less parameters for measurement and operating efficiency were considered. It is fact that the easy implementation of algorithm reduces time to find MPP and does not require advanced microcontroller and noise polluted signals. Moreover, using less parameter decreases hardware complexity. It is know that the most conventional MPPT methods are Perturb & Observe (P&O), Incremental Conductance (IncCon) and Constant Voltage (CV) methods. See flow diagrams for P&O and IncCon at Figure 29 and 30. The first two are so called ‘hill-climbing’ methods, and they are using the fact that on the P - V characteristic, on the left of the MPP the variation of the power against voltage  $dP/dV > 0$ ,

while at the right,  $dP/dV < 0$ . (See Figure 28) [6] The CV method is based on the fact that generally the ratio  $V_{MPP}/V_{OC} \approx 0.76$  [2].

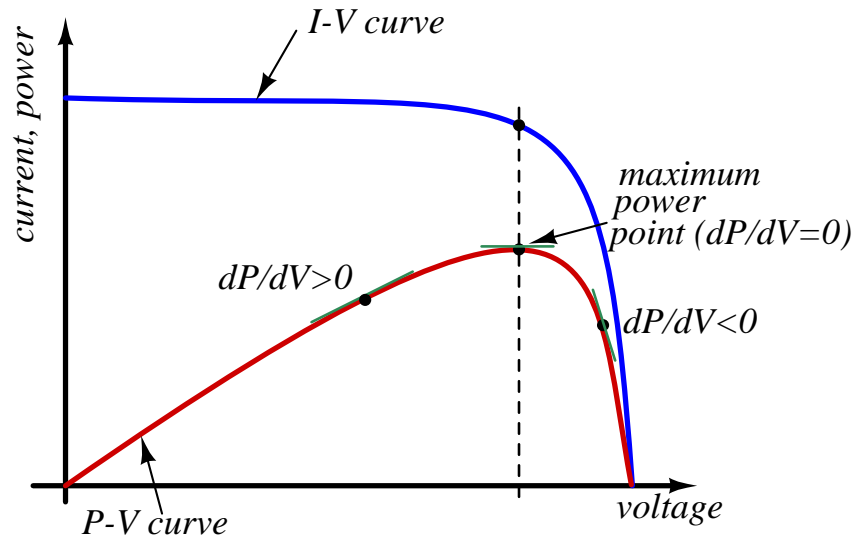


Figure 28: Sign of the  $dP/dV$  at different positions on the power characteristic

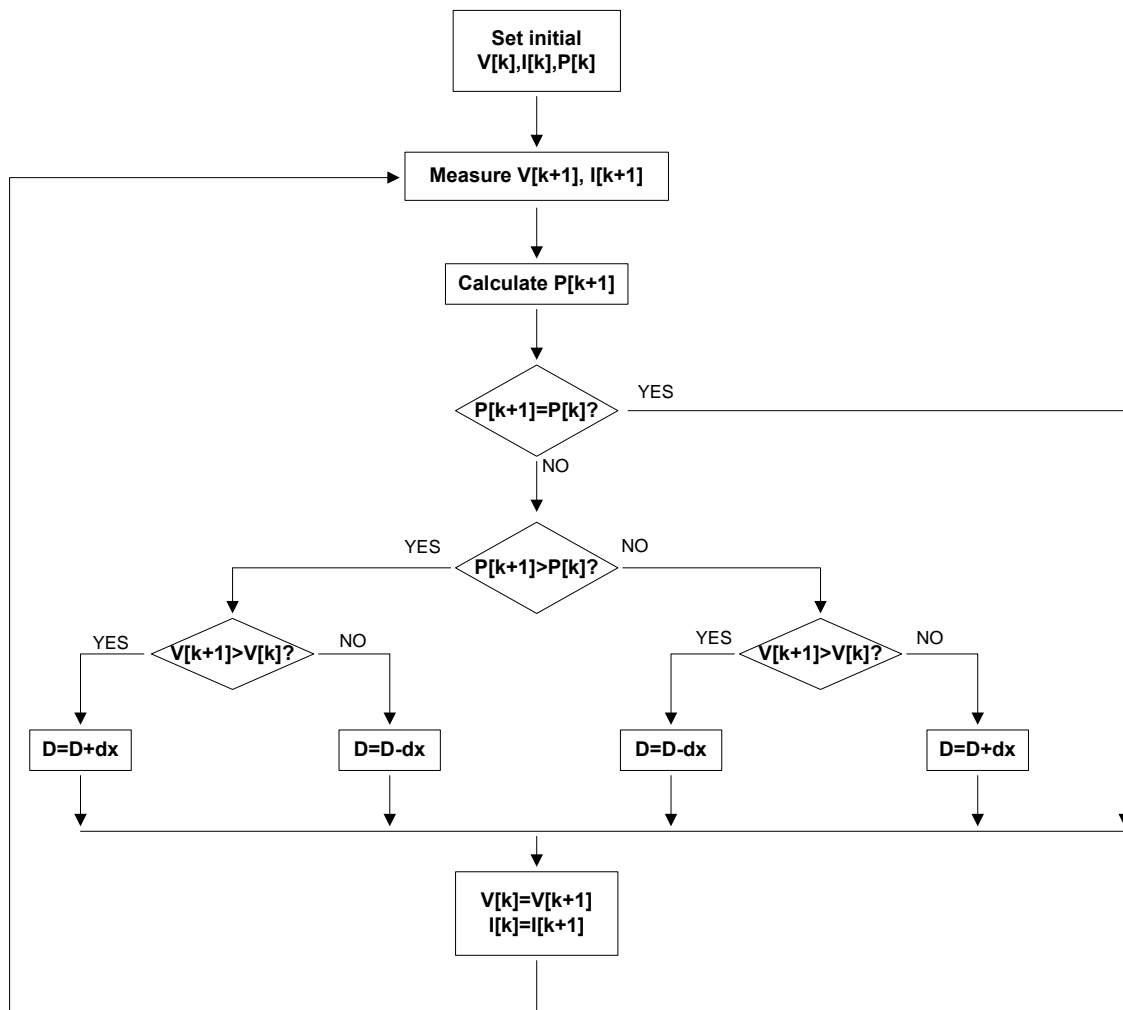


Figure 29: P&O Method Flow Diagram



Figure 30: IncCond Method Flow Diagram

It is obvious that the first two methods require PV operating current and voltage, and the next needs panel open circuit voltage. First, Perturb & Observe (P&O), Incremental Conductance (IncCon) were used as MPPT algorithm. Since it is indicated above that these algorithms using the fact that on the P - V characteristic, it is required to measure current and voltage. To measure current LEM LTS 25 – NP current transducer is used and for voltage a simple voltage divider. It is known that as power conditional circuit buck converter used. The buck converter input current wave for is showed in Figure 31. Moreover, the output signal form of LEM is same as with its input signal. Therefore, the output signal form of LEM is same with form indicated in Figure 31.

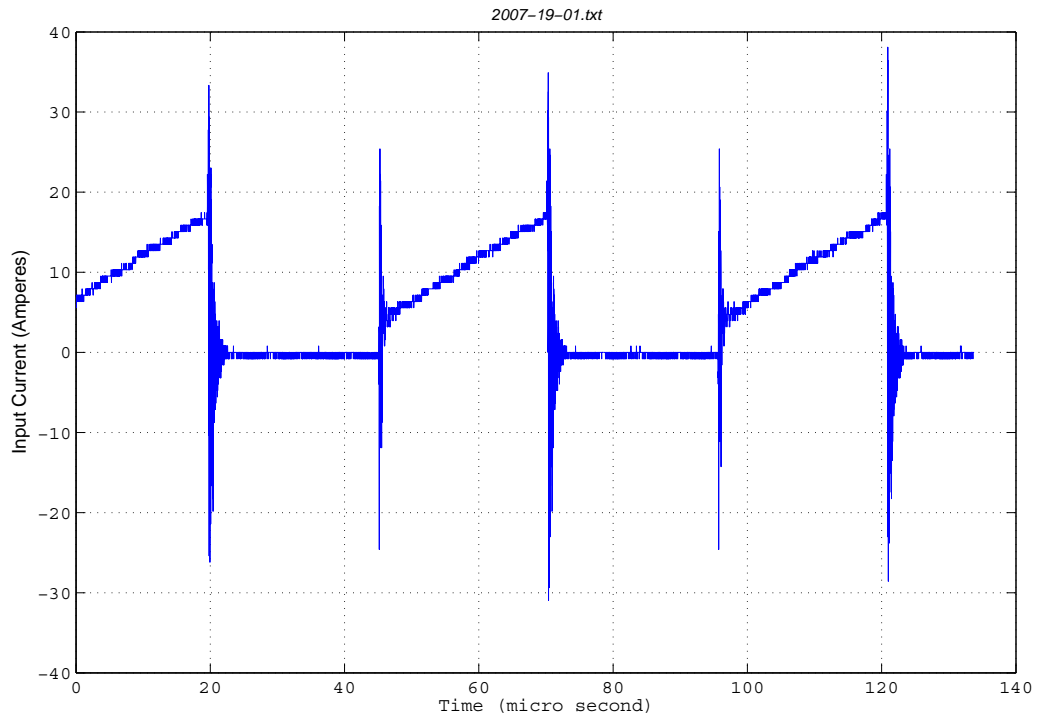


Figure 31: Input Current of MPPT Buck Converter

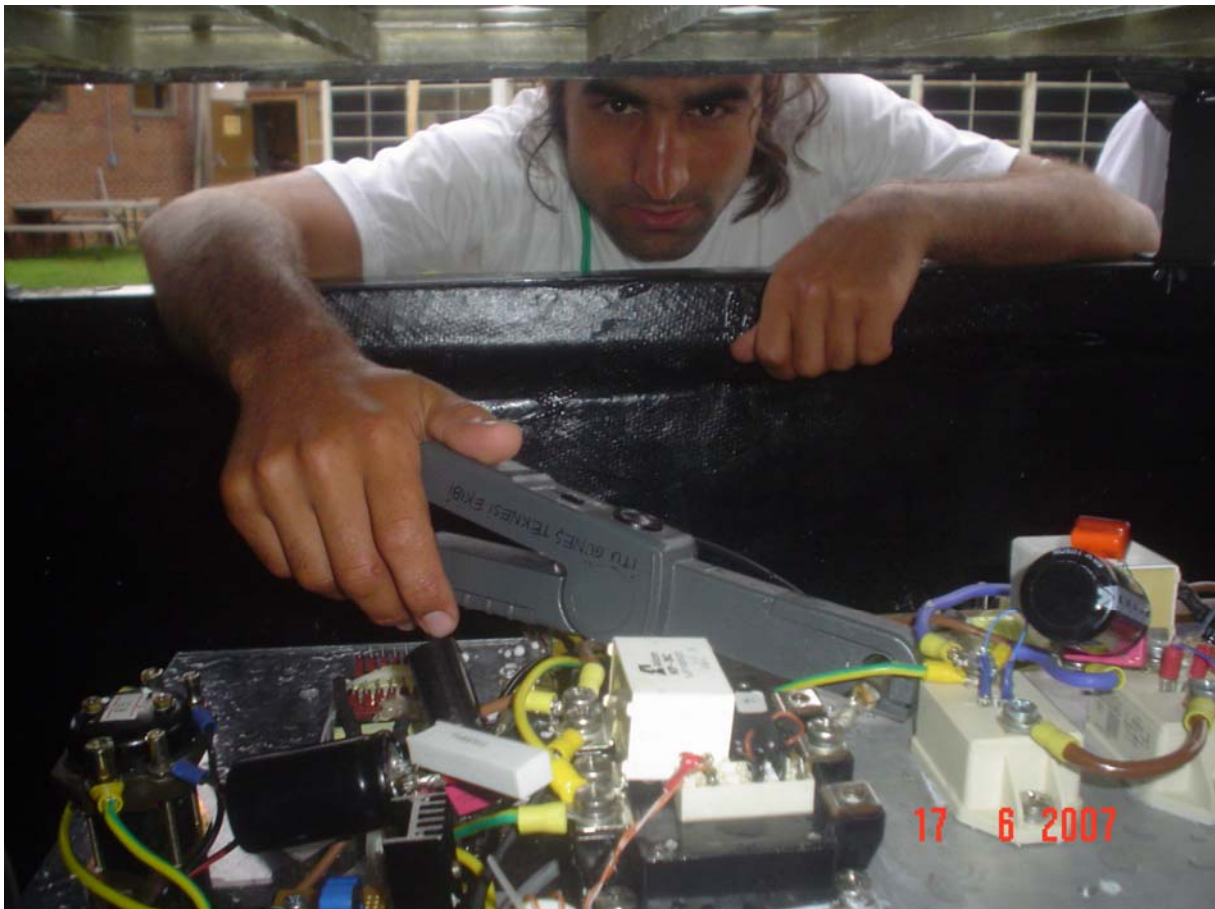


Figure 32: Experimental Test Setup of MPPT Circuit

Moreover, it is fact that for MPPT algorithm an average value is required. Simple low pass passive RC filters were used to take average of LEM output signal. After using various combination of RC, the output signals average was taken (See Figure 31). However, there were oscillations in average output signal. Due to the effect of these spikes MPPT algorithm did not work properly. In order to cope with this problem, second and third order active low pass active RC filters were used. The problems were almost same as with previous. As average output signal of LEM could not be taken properly, it was decided to use passive LC filter. After using it, oscillations were diminished; however, MPPT did not operate properly.

Then, it was decided to use CV method. This method uses the fact that the operating voltage ( $V_{OP}$ ) at MPP of PV-module is near linearly proportional to open circuit voltage ( $V_{OC}$ ) of PV-module.

$$V_{OP} = K \cdot V_{OC}$$

where, the proportional constant (K) is about 0.76 (within  $\pm 2\%$ ). The disadvantage of this method is that the power flows from PV array to load stops for short time to measure open circuit voltage. In other word, the power is not supplied to load during this time and it causes power losses.

In order to solve this problem, the new solution idea was improved. It is known that PV array used for 2007 solar boat consist of serial A- 300 sun cells (See Figure 33). Therefore, if one of A – 300 sun cells' open circuit voltage is measured, the PV array open circuit voltage can be calculated by multiplying the cell voltage with number of series connected cells. By considering this fact, PV array open circuit voltage can be determined by the one sun cell open circuit voltage without disrupting power for short time. Therefore, the array consisting of serially three A – 300 sun cells which was used for ITU Solar Car (See Figure 33). The PV array using different lamination technique is isolated from PV array that supply power for propulsion. In other word, it does not contribute any power to drive the motor or charge the batteries.



Figure 33: Isolated PV array for MPPT Algorithm

Before deciding to use it, there was some hesitation because it has different lamination technique, so it may have different voltage. After measuring all PV arrays at same time during day, there was small difference between them. To reduce difference, the isolated PV array is multiplied by a correction coefficient. The isolated PV array voltage is around 1.65 V. Since the each PV array consists of 28 sun cells, the isolated PV array is multiplied by 28.62 including correlation coefficient. Consequently, the algorithm is designed regarding with 28.62.

In order to control the buck converter duty cycle, the duty cycle of the produced PWM by PIC16F877 is changed. According PIC16F877 datasheet, there are some processes to set PWM properties. After determining PWM frequency, the duty cycle of PWM is changed by CCPR1L register. By changing value of it from 0 to 250, the duty cycle varies from 0% to 100%. Since the isolated PV array voltage less than 5V, ADC reference for PIC, it is not required to use voltage divider. The voltage is measured via ADC of PIC. According to the CV method, the isolated PV array voltage is measured and multiplied by 28.62. After that, the duty cycle is adjusted to set main PV array operating voltage as 76% of open circuit voltage.

The relation between input and output of buck converter is

$$V_{in} = D \times V_{out}$$

where D is duty cycle.

The output voltage of buck converter will be around 24V.

$$V_{out} = 24V \quad (1.19)$$

$$D = \frac{V_{out}}{V_{OV}} \quad (1.20)$$

Where  $V_{OV}$  is operating voltage of main PV array.

$$V_{OV} = 0.76 \times V_{OC} \quad (1.21)$$

$$V_{OC} = V_{is} \times 28.62 \quad (1.22)$$

where  $V_{is}$  is isolated PV array voltage

$$V_{is} = \frac{data \times 5V}{1023} \quad (1.23)$$

where data result of 10 bit ADC as register, its value is changing from 0 to 1023.

$$D = \frac{CCPR1L \times 100}{250} \quad (1.24)$$

By combining Equations 1.19, 1.20, 1.21, 1.22, 1.23 and 1.24, the formula for determining CCPR1L value to adjust PWM duty cycle is:

$$CCPR1L = \frac{84716}{V_{is}} \quad (1.25)$$

Therefore, the MPP can be determined by Eq. 1.25. As it is seen from Eq. 1.25, to determine MPP, required parameter is open circuit voltage of isolated panel. By using this method,

current and voltage measurement does not required. Moreover, due to using just isolated panel voltage, the implementation of algorithm is quite easy.

A pyranometer is used to determine weather the designed algorithm forces main PV array to operate around maximum point or not. A pyranometer is an instrument for measuring total hemispherical solar irradiance on a flat surface, or "global" irradiance (See Figure 34). It is output signal is 100 mV for  $1000 \text{Watt}/\text{m}^2$ . The nominal area of PV array receiving irradiance is  $2.625 \text{m}^2$ .



Figure 34: Pyronometer

### 1.1.3.2 Flow diagram:

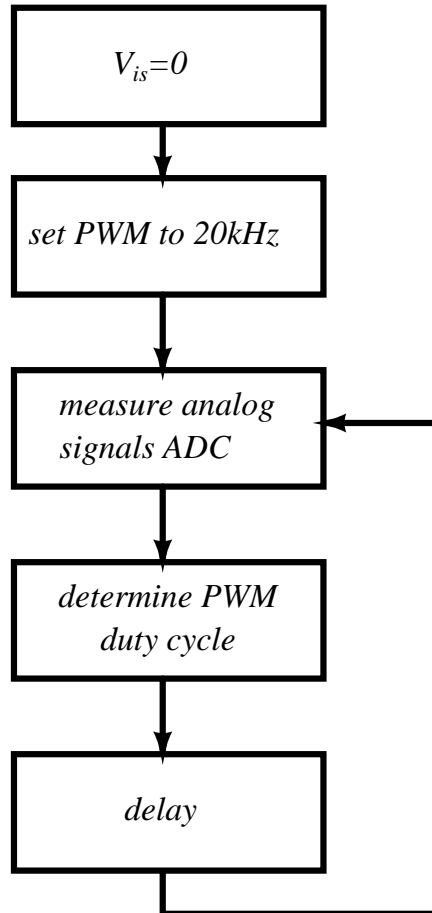


Figure 35: Flow diagram for MPPT

## 2. Conclusion and Future Works

The designed MPPT has worked properly during five days SolarSplash event. The all six for sprint and four for endurance batteries were charged (See Figure 36). Moreover, the MPPT has operated during endurance morning and afternoon laps respectively. During the endurance laps, the PV array current – voltage and batteries current – voltage were measured by telemetry system (See Figure 37). During the laps, the weather was cloudy and a little windy.

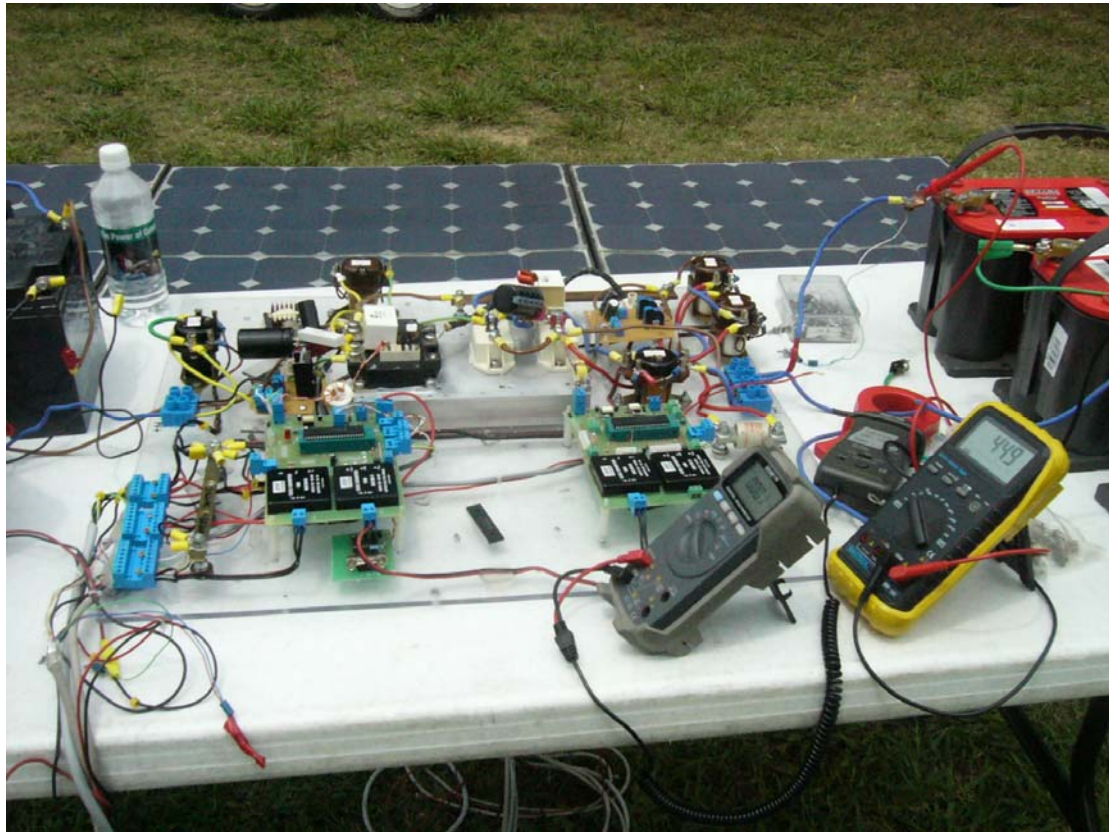


Figure 36: Charging Batteries during Solar Splash event with MPPT

It was seen that the designed MPPT has supplied solar boat requirements. Since, it was the first time to design MPPT and considering maximum efficiency because of being used for the competition, it costed more than a company manufactured MPPT due to drying to find the most efficient form of power electronic circuit and algorithm. As a result, the designed and built MPPT operated properly and can be manufactured by a company cheaply.

Besides, it is obvious that the world energy demand increases everyday and the recent energy sources will have been exhausted in 50 years [7]. That is why the human kind being alerted about this problem tries to improve technology in order to supply energy demand from renewable energy sources. It is know that sun is one of renewable energy sources. The electricity generation by using sun cells widespread as the solar array cost's decreases. As PV array usage widespread, the MPPT requirement will increase.

#### References:

- [1] Weidong Xiao, Dunford W.G.: "A modified adaptive hill climbing MPPT method for photovoltaic power systems" *Power Electronics Specialists Conference, 2004. PESC 04. 2004 IEEE 35th Annual Volume 3*, 20-25 June 2004 Pages: 1957 - 1963 Vol.3
- [2] University of Arkansas Solar Boat Team, Solar Splash Competition Technical Report, 2006
- [3] Weidong Xiao, Dunford W.G.: "A modified adaptive hill climbing MPPT method for photovoltaic power systems" *Power Electronics Specialists Conference, 2004. PESC 04. 2004 IEEE 35th Annual Volume 3*, 20-25 June 2004 Pages: 1957 - 1963 Vol.3

[4] Erickson, R.W., Supplementary notes on EMI and Layout Fundamentals for switched mode Circuits, ECEN 5797 Power Electronics 1 Lecture notes

[5] Tweedie, S., “Experimental Investigation of Flow Control Techniques To Reduce Hydroacoustic Rotor-Stator Interaction Noise”, 2006

[6] Hohm D.P., Ropp M.E.: “Comparative Study of Maximum Power Point Tracking Algorithms Using an Experimental, Programmable, Maximum Power Point Tracking Test Bed”. *Photovoltaic Specialists Conference, 2000. Conference Record of the Twenty-Eighth IEEE* 15-22 Sept. 2000 Pages:1699 – 1702

[7] [www.usenergyagency.org](http://www.usenergyagency.org)

[8] Demirok, E., Graduation Project “Maximum Power Point Tracker”, 2005

## Appendix

### C Codes

#### Delay.h

```
/*
 * Delay functions for HI-TECH C on the PIC
 *
 * Functions available:
 *     DelayUs(x)  Delay specified number of microseconds
 *     DelayMs(x)  Delay specified number of milliseconds
 *
 * Note that there are range limits: x must not exceed 255 - for xtal
 * frequencies > 12MHz the range for DelayUs is even smaller.
 * To use DelayUs it is only necessary to include this file; to use
 * DelayMs you must include delay.c in your project.
 */

/*
 * Set the crystal frequency in the CPP predefined symbols list in
 * HPDPIC, or on the PICC command line, e.g.
 * picc -DXTAL_FREQ=4MHZ
 *
 * or
 * picc -DXTAL_FREQ=100KHZ
 *
 * Note that this is the crystal frequency, the CPU clock is
 * divided by 4.
 *
 * MAKE SURE this code is compiled with full optimization!!!
 */

#ifndef XTAL_FREQ
#define XTAL_FREQ 4MHZ      /* Crystal frequency in MHz */
#endif

#define MHZ *1000L          /* number of kHz in a MHz */
#define KHZ *1              /* number of kHz in a kHz */

#if XTAL_FREQ >= 12MHZ

#define DelayUs(x) { unsigned char _dcnt; \
                    _dcnt = (x)*((XTAL_FREQ)/(12MHZ)); \
                    while(--_dcnt != 0) \
                        continue; }

#else

#define DelayUs(x) { unsigned char _dcnt; \
                    _dcnt = (x)/((12MHZ)/(XTAL_FREQ))|1; \
                    while(--_dcnt != 0) \
                        continue; }

#endif

extern void DelayMs(unsigned char);
```

#### Delay.c

```

/*
 * Delay functions
 * See delay.h for details
 *
 * Make sure this code is compiled with full optimization!!!
 */

#include "delay.h"

void
DelayMs(unsigned char cnt)
{
#if XTAL_FREQ <= 2MHZ
    do {
        DelayUs(996);
    } while(--cnt);
#endif

#if XTAL_FREQ > 2MHZ
    unsigned char i;
    do {
        i = 4;
        do {
            DelayUs(250);
        } while(--i);
    } while(--cnt);
#endif
}

```

## Main.c

```

#include <stdio.h>
#include "pic.h"
#include "delay.h"
#include "delay.c"

#define MAX 10
#define LIMIT 50

typedef void VOID;
typedef int INT;
typedef signed char INT8;
typedef signed int INT16;
typedef signed long INT32;
typedef unsigned short WORD;
typedef char CHAR;
typedef unsigned char BYTE;
typedef float FLOAT;
typedef double DOUBLE;
typedef long LONG;
typedef INT8 BOOL;

#define FOSC (20000000L)
#define SCI_EIGHT (0)
#define SCI_NINE (1)

#define AN0 0

```

```

#define AN1 1
#define AN2 2
#define AN3 3
#define AN4 4
#define AN5 5
#define AN6 6
#define AN7 7

#define VAR 10
#define SAMPLE 30

unsigned char g_adc[MAX] = "";

unsigned char
sci_Init(unsigned long int baud, unsigned char ninebits)
{
    int X;
    unsigned long tmp;

    /* calculate and set baud rate register */
    /* for asynchronous mode */
    tmp = 16UL * baud;
    X = (int)(FOSC/tmp) - 1;
    if((X>255) || (X<0))
    {
        tmp = 64UL * baud;
        X = (int)(FOSC/tmp) - 1;
        if((X>255) || (X<0))
        {
            return 1; /* panic - baud rate unobtainable */
        }
        else
            BRGH = 0; /* low baud rate */
    }
    else
        BRGH = 1; /* high baud rate */
    SPBRG = X; /* set the baud rate */

    SYNC = 0; /* asynchronous */
    SPEN = 1; /* enable serial port pins */
    CREN = 1; /* enable reception */
    SREN = 0; /* no effect */
    TXIE = 0; /* disable tx interrupts */
    RCIE = 0; /* disable rx interrupts */
    TX9 = ninebits?1:0; /* 8- or 9-bit transmission */
    RX9 = ninebits?1:0; /* 8- or 9-bit reception */
    TXEN = 1; /* enable the transmitter */

    return 0;
}

void
sci_PutByte(unsigned char byte)
{
    while(!TXIF) /* set when register is empty */
        continue;
    TXREG = byte;

    return;
}

unsigned char

```

```

sci_GetByte(void)
{
    while(!RCIF)      /* set when register is not empty */
        continue;

    return RCREG;     /* RXD9 and FERR are gone now */
}

int ADC(unsigned decimal,unsigned n_sample)//should select according bit
order
{
    unsigned int i;
    unsigned short int data = 0;
    int result = 0;
    unsigned char adc[MAX];

    PORTA = 0;
    TRISA = 255;

    PORTE = 0;
    TRISE = 255;

    result = 0;
    data = 0;

    for(i = 0; i < n_sample;i++) {
        ADCON1 = 192;// 11000000 AD result select bit.rigth justify(7) -
Fosc/64(6) - all analog channel ad port configuration bit...VDD is
Vref(3,2,1,0,9)
        ADCON0 = 129;// 10000001 Fosc/64 - AD conversion select channel AN0
- turn on A/D module -
        switch(decimal) {

            case 0:
                break;
            case 1:
                ADCON0 |= 8;//AN1 selected
                break;
            case 2:
                ADCON0 |= 16;//AN2selected
                break;
            case 3:
                ADCON0 |= 24;//AN3selected
                break;
            case 4:
                ADCON0 |= 32;//AN4selected
                break;
            case 5:
                ADCON0 |= 40;//AN5selected
                break;
            case 6:
                ADCON0 |= 48;//AN6selected
                break;
            case 7:
                ADCON0 |= 56;//AN7selected
                break;
            default :
                break;
        }

        DelayUs(100);
        ADCON0 |= 4;//00000100 start conversion.set AD/DONE ADCON0 bit
    }
}

```

```

        while(ADCON0 & 4)//wait adc convert is complete by AD/DONE bit to
be cleared
            ;//polling
                data = ADRESH;
                    data = data << 8;
                    data |= ADRESL;
result += data;
}

result /= i;

return result;
}

void SetPWM(void)
{
    TRISC = 249;//bit 2 and 1 is set as output while the others input
    PR2 = 249;//period is determined 20kHz with 1 prescaler
    T2CON |= 4;// prescaler is 1 and TMR is on
    CCP1CON |= 12;//CCP1 is PWM
}

void SendData(unsigned char *str)
{
    int i;

    for(i = 0; str[i] != '\0';i++) { // sending data
        sci_PutByte(str[i]);
        str[i] = "";
    }
    str[i] = "";
}

void Delay(unsigned int n)
{
    int i;

    for(i = 0;i < n;i++)
        DelayMs(255);
}

void main()
{
    int DC = 145,flag = 0;
    unsigned short int dx0 = 2,dx1 = 4,dx2 = 6;
    int V1 = 0, I1 = 0, V0 = 0,I0 = 0,i,P1 = 0,P0 = 0,Vpiro = 0,Vpvt =
0,Imppt = 0, manuel = 0;

    TRISB7 = 0;

    sci_Init(19200, SCI_EIGHT); // initilizing serial port
    SetPWM();// setting PWM
    CCP1L = DC;
    while(1){
        RB7 = 1;

```

```

manuel = ADC(AN6,5);
if(manuel > LIMIT) {
    manuel = (manuel / 4 - 6); // manuel control section, the
CCPR1L shall not exceed 249.
    if(manuel < 0)
        manuel = 0;
CCPR1L = manuel;
}

else {
Vpvt = ADC(AN2,10); // kenux control
CCPR1L = 84716/Vpvt; //58000(kenux constant) for 36V
}

I1 = ADC(AN0,5) - 510; // panel current
if(I1 < 0)
    I1 = 0;
V1 = ADC(AN1,5); // panel voltage
I0 = ADC(AN3,5); // battery voltage
V0 = ADC(AN5,5); // battery current
Imppt = ADC(AN7,5) - 510; // mppt output current
if(Imppt < 0)
    Imppt = 0;

RB7 = 0;

sprintf(g_adc, "?%d_%d_\0", I1, V1);
SendData(g_adc);
sprintf(g_adc, "%d_%d_\0", I0, V0);
SendData(g_adc);
sprintf(g_adc, "%d_%d_\0", Imppt, Vpvt);
SendData(g_adc);
sprintf(g_adc, "%d_0!\0", CCPR1L);
SendData(g_adc);

RB7 = 1;

}
}

```